

# SkM1 and Cx32 improve conduction in canine myocardial infarcts yet only SkM1 is antiarrhythmic

Gerard J.J. Boink<sup>1,2,3,4</sup>, David H. Lau<sup>1</sup>, Iryna N. Shlapakova<sup>1,5</sup>, Eugene A. Sosunov<sup>1,2</sup>, Evgeny P. Anyukhovskiy<sup>1,2</sup>, Helen E. Driessen<sup>1,6</sup>, Wen Dun<sup>1</sup>, Ming Chen<sup>1</sup>, Peter Danilo Jr<sup>1,2</sup>, Tove S. Rosen<sup>7</sup>, Nazira Özgen<sup>1</sup>, Heather S. Duffy<sup>1,8</sup>, Yelena Kryukova<sup>1</sup>, Penelope A Boyden<sup>1,2</sup>, Richard B. Robinson<sup>1,2</sup>, Peter R. Brink<sup>9</sup>, Ira S. Cohen<sup>9</sup>, and Michael R. Rosen<sup>1,2,7,9\*</sup>

<sup>1</sup>Department of Pharmacology, Columbia University, 630 West 168 Street, PH 7W-321, New York, NY 10032, USA; <sup>2</sup>Center for Molecular Therapeutics, Columbia University, 630 West 168 Street, PH 7W-321, New York, NY 10032, USA; <sup>3</sup>Interuniversity Cardiology Institute of the Netherlands (ICIN), Utrecht, The Netherlands; <sup>4</sup>Heart Failure Research Center, Academic Medical Center, University of Amsterdam, Amsterdam, The Netherlands; <sup>5</sup>Operating Room RN, Meadowlands Hospital Medical Center, 55 Meadowlands Parkway, Secaucus, NJ 07094, USA; <sup>6</sup>Graduate School of Life Sciences, Utrecht University, Utrecht, The Netherlands; <sup>7</sup>Department of Pediatrics, Columbia University, 630 West 168 Street, PH 7W-321, New York, NY 10032, USA; <sup>8</sup>Beth Israel Deaconess Medical Center, Harvard Medical School, Center for Life Sciences, CLS 913, 3 Blackfan Circle, Boston, MA 02115, USA; and <sup>9</sup>Department of Physiology and Biophysics, Institute for Molecular Cardiology, Stony Brook University, Stony Brook, NY, USA

Received 23 August 2011; revised 20 February 2012; accepted 23 February 2012; online publish-ahead-of-print 27 February 2012

Time for primary review: 13 days

<b>Aims</b>	Reentry accounts for most life-threatening arrhythmias, complicating myocardial infarction, and therapies that consistently prevent reentry from occurring are lacking. In this study, we compare antiarrhythmic effects of gene transfer of green fluorescent protein (GFP; sham), the skeletal muscle sodium channel (SkM1), the liver-specific connexin (Cx32), and SkM1/Cx32 in the subacute canine infarct.
<b>Methods and results</b>	Immediately after ligation of the left anterior descending artery, viral constructs were implanted in the epicardial border zone (EBZ). Five to 7 days later, efficient restoration of impulse propagation (narrow QRS and local electrogram duration) occurred in SkM1, Cx32, and SkM1/Cx32 groups ( $P < 0.05$ vs. GFP). Programmed electrical stimulation from the EBZ induced sustained ventricular tachycardia (VT)/ventricular fibrillation (VF) in 15/22 GFP dogs vs. 2/12 SkM1, 6/14 Cx32, and 8/10 SkM1/Cx32 ( $P < 0.05$ SkM1 vs. GFP). GFP, SkM1, and SkM1/Cx32 had predominantly polymorphic VT/VF, whereas in Cx32 dogs, monomorphic VT predominated ( $P < 0.05$ for Cx32 vs. GFP). Tetrazolium red staining showed significantly larger infarcts in Cx32- vs. GFP-treated animals ( $P < 0.05$ ).
<b>Conclusion</b>	Whereas SkM1 gene transfer reduces the incidence of inducible VT/VF, Cx32 therapy to improve gap junctional conductance results in larger infarct size, a different VT morphology, and no antiarrhythmic efficacy.
<b>Keywords</b>	Myocardial infarction • Arrhythmias • Na <sup>+</sup> channels • Connexins • Gene therapy

## 1. Introduction

Reentry is the predominant mechanism for arrhythmias complicating ischaemic heart disease.<sup>1,2</sup> These arrhythmias are facilitated by slow conduction and their prevention has focused on strategies that create bidirectional conduction block (Na<sup>+</sup> channel blocker, surgery, or ablation) and/or prolong refractoriness.<sup>3</sup> Alternatively, reentry may be averted by speeding conduction such that the reentrant wave front encounters its own refractory tail. While catecholamines and muscarinic agonists can be used to hyperpolarize the cell

membrane and speed conduction, they have proarrhythmic and toxic properties that contravene their use. More recently, the gap junction-specific peptide rotigaptide has been explored as a novel antiarrhythmic strategy. Although rotigaptide facilitated rapid impulse propagation and reduced the incidence of spontaneous ischaemia/reperfusion-based arrhythmias,<sup>4</sup> these effects could not be reproduced in the permanently ischaemic epicardial border zone (EBZ).<sup>5</sup>

EBZs overlying infarcts manifest membrane depolarization facilitating slow conduction and reentry. Previously, we have overexpressed SkM1 (SCN4A), a sodium channel that functions more effectively at

\* Corresponding author. Tel: +1 212 305 8754; fax: +1 212 305 8351, Email: mrr1@columbia.edu

depolarized potentials than cardiac SCN5A in EBZ of canine infarcts. This resulted in increased  $V_{\max}$  of the action potential (AP), more rapid longitudinal conduction velocity,<sup>6</sup> and reduced incidence of ventricular tachycardia (VT)/ventricular fibrillation (VF) initiated by programmed electrical stimulation (PES) in the healing infarct.<sup>7</sup> A comparable result was obtained for spontaneous VT/VF in a murine ischaemia/reperfusion model.<sup>8</sup>

Another potential strategy to optimize EBZ conduction is the maintenance/improvement of gap junction coupling. The reduced pH of ischaemic tissue results in closure of Cx43 (predominant ventricular isoform) gap junctions, contributing to slow conduction and reentry.<sup>9,10</sup> The liver-specific isoform, Cx32, largely remains open upon acidification and may therefore provide a means to maintain fast conduction and prevent reentry.<sup>11</sup> Adenoviral delivery of Cx32 (Ad-Cx32) in the murine ischaemia–reperfusion model revealed antiarrhythmic efficiency similar to that of Ad-SkM1.<sup>8</sup> A potential concern with Cx32 overexpression is that it can promote intercellular transmission of biochemical mediators of injury and thereby increase infarct size. Reinforcing this concern, we found that in mice overexpressing Cx32, infarct size was increased.<sup>12</sup>

To increase our understanding of antiarrhythmic strategies that speed conduction, we now compared SkM1-, Cx32-, and SkM1/Cx32-based approaches in their ability to speed conduction in the canine EBZ and to modify or prevent VT/VF induction. In addition, we related infarct size to the genetic interventions, incidence and expression of arrhythmias, and used immunohistochemical and tissue bath studies to confirm and compare the presence and functionality of the overexpressed genes.

## 2. Methods

### 2.1 Adenovirus preparation

Rat SkM1 and murine Cx32 adenovirus were prepared as described previously.<sup>7,8</sup> Briefly, replication-deficient adenoviruses of SkM1, Cx32, and green fluorescent protein (GFP) were plaque-purified and large-scale viral stocks were concentrated via CsCl binding, and subsequently titrated with mouse anti-adenovirus hexon antibodies (Advanced ImmunoChemical, Long Beach, CA, USA). The titre was defined in fluorescent focus-forming units (ffu) per millilitre (ffu/mL).

### 2.2 Intact animal and isolated tissue methods

The investigation conforms with the Guide for the Care and Use of Laboratory Animals published by the US National Institutes of Health (NIH Publication No. 85-23, revised in 1996) and the protocols were reviewed and approved by the Columbia University Animal Care and Use Committee.

### 2.3 Canine infarct preparation and adenovirus injection

Adult male mongrel dogs (22–25 kg; Chestnut Ridge Kennels, Shippensburg, PA, USA) were anaesthetized with thiopental (17 mg/kg iv) and mechanically ventilated. Anaesthesia was maintained with isoflurane (1.5–3.0%). The depth of anaesthesia was monitored by a veterinary anaesthesia technician throughout all surgical procedures. Systemic arterial blood pressure and a body surface electrocardiogram (ECG) were continuously monitored intraoperatively. Increases in heart rate and blood pressure >20% of initial values were used to indicate the need for increases in isoflurane levels. In addition, palpebral or corneal reflexes were monitored.

A left thoracotomy was performed using sterile techniques, and sites of coronary ligation were selected on the basis of the distribution of the left anterior descending artery and collateral circulation from the left circumflex.<sup>13</sup> Adenoviral constructs expressed GFP (designated Ad-GFP) SkM1/GFP (designated Ad-SkM1), Cx32/GFP (designated Ad-Cx32), or SkM1/Cx32 (designated Ad-SkM1/Cx32).  $6 \times 10^{10}$  ffu of each in 0.8 mL solution divided into four separate aliquots was injected within 5 mm of one another in a square array into the EBZ at selected wide electrogram (EG) sites at 1–2 mm depth with a modified Hamilton (30 G) syringe. The chest was closed, lidocaine infusion (50 µg/kg/min) was initiated during surgery, and prophylactic lidocaine continued for 24–48 h postoperatively. At 5–7 days of recovery, dogs were anaesthetized, the heart was exposed, and ECGs and EGs were acquired, digitized, and stored on a personal computer (EMKA Technologies, Falls Church, VA, USA). Studies were terminated at days 5–7 because this is during the subacute infarct period and because it provides a time window of plateau adenoviral gene expression during which we have shown SkM1 gene transfer to protect efficiently against arrhythmia induction.<sup>5</sup>

The dose of  $6 \times 10^{10}$  fluorescent focus-forming units (ffu) of each vector employed in the present study (the GFP group received a double dose to keep the number of viral particles administered equal) was chosen for consistency with previous studies<sup>7</sup> and also because unpublished pilot studies indicated a higher dose of  $1.2 \times 10^{11}$  ffu to be associated with an excessive inflammatory/toxic response. In these earlier pilot studies, both Ad-GFP-injected animals and Ad-SkM1-injected animals showed high levels of transgene expression in immunohistochemical experiments. Yet, histology showed excessive cell death and a high degree of immune cell infiltration. Upon electrophysiological examination, no normalization of fast impulse propagation was found in either of the two groups (based on the measurements of QRS duration and local EGs), and all animals had inducible VT/VF. Finally, tissue bath experiments were in general not feasible due to the overall poor tissue quality of the epicardial samples taken from the injection site.

Arrhythmia induction outcomes for a subset of the animals injected with Ad-GFP ( $n=9$ ) and all animals injected with Ad-SkM1 ( $n=12$ ) have been reported previously<sup>7</sup>; yet, for these previously reported animals, we have now added additional analysis of ECG parameters and QRS duration during premature stimulation. An additional 15 animals were injected with Ad-GFP and studied concurrently with the animals injected with Ad-Cx32 ( $n=15$ ) and Ad-SkM1/Cx32 ( $n=10$ ). The study of the initial series of Ad-GFP and Ad-SkM1 animals (studied in 2007–08) was immediately followed by the Ad-GFP, Ad-Cx32, and Ad-SkM1/Cx32 groups (studied by the same team in 2008–09).

### 2.4 VT induction

Pacing threshold was determined by incrementally increasing the current until ventricular capture occurred; pacing was then performed at  $2 \times$  pacing threshold. Extrastimulus pacing with a programmable stimulator (Bloom Associates, Reading, PA, USA) was performed sequentially in the high ventricular septum, infarct lateral border zone, viral injection site, and within the infarct. Pacing trains began with 10 stimuli at a cycle length of 350–400 ms. S2 was initiated at 250 ms, and S1–S2 was decreased in 5 ms steps until loss of capture. For S3 pacing, S1–S2 was set at the shortest interval with reliable S2 capture [equivalent to the effective refractory period (ERP)]. S3 was initiated at an initial coupling interval of 100 ms and increased in 10 ms steps until S3 capture occurred. If VT lasted  $\geq 60$  s, the heart was removed and prepared for microelectrode study, histology, and infarct sizing.

### 2.5 Microelectrode methods

Hearts were removed and immersed in a previously described Tyrode's solution<sup>14</sup> equilibrated with 95% O<sub>2</sub>/5% CO<sub>2</sub>. Epicardial strips ( $\approx 10 \times 5 \times 0.5$ –1 mm) were filleted parallel to the left ventricular free wall surface from infarct sites injected with SkM1, Cx32, and/or GFP, from

infarcted non-injected sites, and from the normal myocardium. Preparations were pinned to the bottom of a 4 mL tissue bath (epicardial surface up) and superfused ( $36^{\circ}\text{C}$ ,  $\text{pH } 7.35 \pm 0.05$ ) at 12 mL/min with Tyrode's solution containing (in mmol/L): NaCl 131,  $\text{NaHCO}_3$  18, KCl 4,  $\text{CaCl}_2$  2.7,  $\text{MgCl}_2$  0.5,  $\text{NaH}_2\text{PO}_4$  1.8, and dextrose 5.5. Preparations were paced at a cycle length of 500 ms, and APs were recorded during 30–50 impalements per preparation after 3 h of equilibration to reach steady state.<sup>14</sup> The activation time of each impalement site was determined as the time interval between stimulus artefact and AP upstroke. Activation maps were created from sequential impalements of the tissue slabs superfused at potassium concentrations of 4 and 7 mmol/L (to simulate ischaemia-induced membrane depolarization). We also varied pH to simulate ischaemia-induced acidification. Intracellular acidification was studied using an HEPES-buffered Tyrode's solution containing (mmol/L): NaCl 130, KCl 4,  $\text{CaCl}_2$  1.8,  $\text{MgCl}_2$  1.0, dextrose 5.5, sodium acetate 20, and HEPES 10 ( $\text{pH } 7.4$ ). For the low pH solution ( $\text{pH } 6.0$ ), HEPES was replaced by 2-*N*-morpholino-ethanesulfonic acid buffer (10 mmol/L). Acetate, a weak acid that shuttles  $\text{H}^+$  by diffusing through the plasma membrane in its neutral  $\text{H}^+$ -associated form, allows significant reduction in intracellular pH.<sup>15</sup> Preparations were equilibrated for 15 min after a superfusate was changed.

## 2.6 Infarct sizing

After epicardial tissues were removed for microelectrode study and histology, the heart was cooled to  $4^{\circ}\text{C}$  and cut into 1 cm-thick transverse slices from the apex to the base. Slices were incubated for 20 min in 1% tetrazolium red ( $\text{pH } 7.4$  buffer at  $37^{\circ}\text{C}$ ), immersed in 10% formalin for 15 min, and pressed between two glass plates to obtain uniform 1 cm thickness. Apical sides of slices were photographed, and a digital image was obtained. Planimetry (Image J Analysis 1.40 g, National Institutes of Health, Bethesda, MD, USA) was used to determine overall infarct size. The volume of the infarcted myocardium was calculated by multiplying planimetered areas by slice thickness and expressed as per cent total left ventricular volume.

## 2.7 Histology and immunohistochemistry

Evidence of SkM1 and Cx32 overexpression was validated in injected animals by immunohistochemistry. Tissue blocks were snap-frozen in liquid nitrogen, and  $5\ \mu\text{m}$  serial sections were cut with a cryostat (Microm HM505E) and air dried. Sections were washed in phosphate-buffered saline, blocked for 20 min with 10% goat serum, and incubated overnight at  $4^{\circ}\text{C}$  with anti-SkM1 (1:200, Sigma-Aldrich) and/or anti-Cx32 antibodies (1:200, Zymed Laboratories-Invitrogen) and anti-Cx43 antibodies (1:200, Invitrogen). Antibody bound to target antigen was detected by incubating sections for 2 h with goat anti-mouse IgG labelled with Cy3 (red fluorescence for Cx32) and goat anti-rabbit IgG labelled with Alexa 488 (green fluorescence for SkM1 or Cx43); images were collected with a Nikon E800 fluorescence microscope. SkM1 and Cx32 were detected only in animals that had received the corresponding adenovirus (Figure 1). Based on these immunohistochemistry studies, we estimate that  $\sim 50\%$  of EBZ cardiac myocytes were transduced with the gene constructs used. The presence of overexpressed Skm1 and Cx32 in the intercalated disk region of cardiac myocytes has previously been reported<sup>6,8</sup> and was further confirmed in the Supplementary material online, Figures S2 and S3.

## 2.8 Statistical analysis

Data are expressed as mean  $\pm$  SEM. Arrhythmia incidence (the ability of PES to induce sustained VT) and arrhythmia morphology (monomorphic vs. polymorphic) were analysed by  $\chi^2$  test. Difference in ECG parameters, EG width, ERP, and *in vitro* AP parameters were analysed by one-way ANOVA followed by Bonferroni's *post hoc* test. QRS duration during premature stimulation, *in vitro* conduction velocities, and  $V_{\text{max}}$  curves were

analysed with two-way ANOVA followed by Bonferroni's post-tests. Values of  $P < 0.05$  were considered significant.

The authors had full access to and take full responsibility for the integrity of the data. All authors have read and agree to the manuscript as written.

## 3. Results

### 3.1 Intact animal studies

Twenty-four dogs were injected with Ad-GFP, 12 with Ad-SkM1, 15 with Ad-Cx32, and 10 with Ad-SkM1/Cx32. One animal died during surgery (Ad-Cx32) and two died within 2 days after surgery (Ad-GFP); all of arrhythmias. These animals were excluded from further analysis. On days 5–7, we evaluated ECGs and performed terminal *in situ* and *in vitro* experiments. During sinus rhythm, heart rate, PR, QT, and QTc intervals did not differ among groups (Table 1). However, QRS duration in the SkM1, Cx32, and SkM1/Cx32 groups was shorter than in GFP-injected animals ( $P < 0.05$ ; Table 1). Furthermore, during epicardial mapping of the EBZ, we detected broad, fragmented EGs in GFP-injected animals, whereas EGs were short and unfragmented in the SkM1, Cx32, and SkM1/Cx32 groups (Table 1 and Figure 2).

We also studied QRS duration and ERP during premature stimulation. ERP did not differ among groups regardless of the stimulation site (Table 1). Premature stimulation from the paraseptal (PS) or the EBZ injection sites resulted in shorter QRS durations in the SkM1, Cx32, and SkM1/Cx32 groups vs. the GFP group ( $P < 0.05$ ; Figure 3). QRS duration in the SkM1/Cx32 group was also shorter than in the SkM1 and Cx32 groups ( $P < 0.05$ ; Figure 3) during EBZ site stimulation.

### 3.2 Induction and expression of VT/VF

Despite the efficient shortening of QRS and EG durations in all therapeutic groups, consistent with more rapid conduction, arrhythmia induction outcomes differed. Figure 4A illustrates typical outcomes for each group. PES induced VT/VF in the majority of GFP-treated animals (68%) and this incidence was reduced to 17% in the SkM1 group ( $P < 0.05$ ; Figure 4B). It should be noted that the incidence of VT/VF in response to PES within the Ad-GFP group has historically been 65–75% within our laboratory and this does not differ from the incidence of 70% we found in 10 infarcted and non-injected animals that we reported in a separate series of experiments.<sup>16</sup> The incidence of inducible VT/VF was 43% for Cx32 and 80% for SkM1/Cx32 ( $P < 0.05$  vs. the SkM1 group); neither differed from the GFP group ( $P > 0.05$ ).

Importantly, the arrhythmias in Cx32-injected animals were primarily monomorphic and this was significantly different from the predominant polymorphic VT of the GFP group ( $P < 0.05$ ; Figure 4B). Whereas the polymorphic VT rapidly progressed to VF, the majority of monomorphic VT was stable. In three of three GFP, four of five Cx32, and one of one SkM1/Cx32-injected animals in which we attempted to entrain the arrhythmias, they were captured by overdrive pacing and terminated by slowing the pacing rate. Figure 5A illustrates the termination of a monomorphic VT in a Cx32-treated animal.

### 3.3 Infarct size

Infarct sizes were comparable in the GFP, SkM1, and SkM1/Cx32 groups. The Cx32 group had larger infarcts ( $P < 0.05$  vs. GFP;

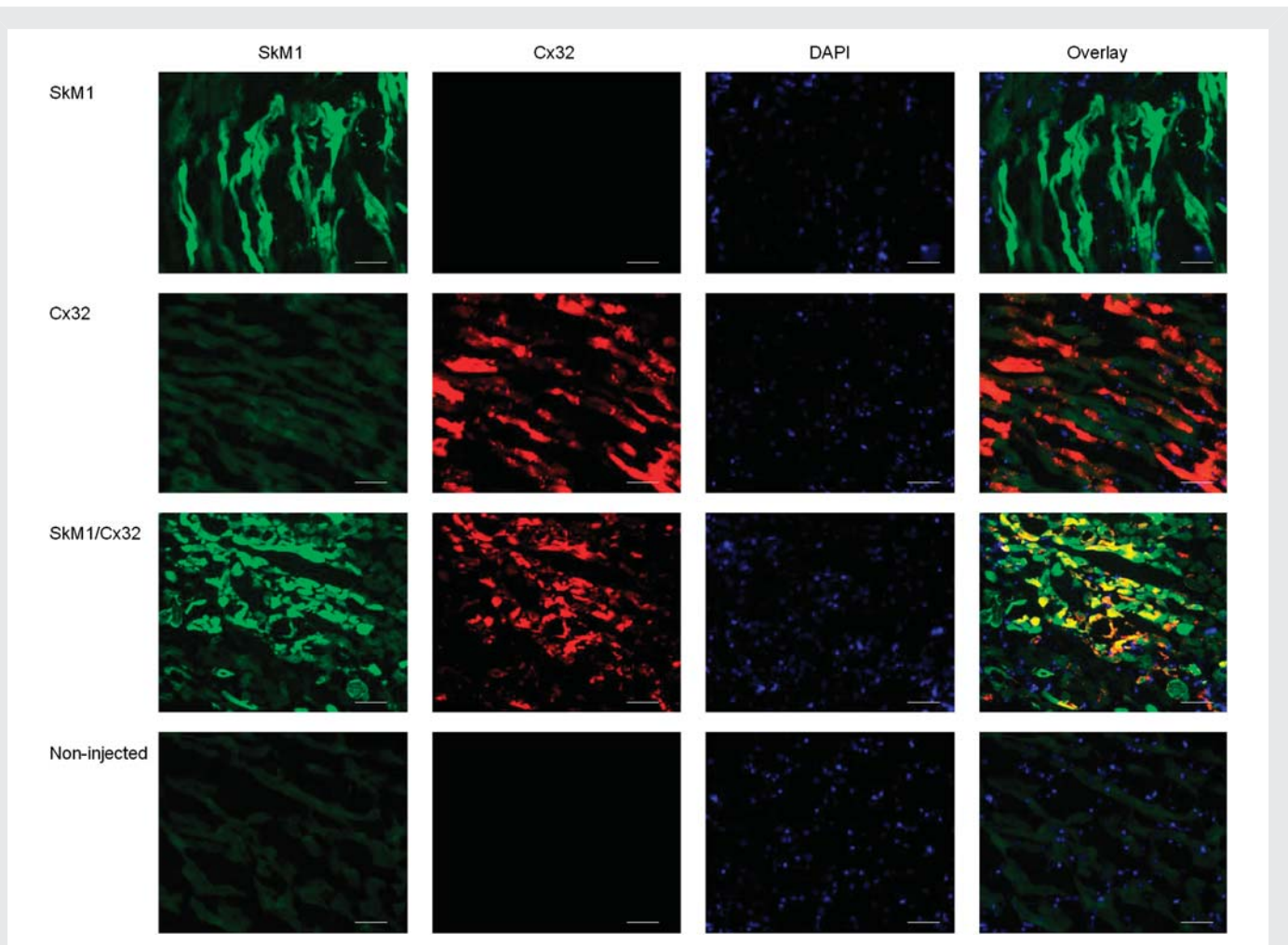


**Figure 1** Immunohistochemistry of the EBZ. Positive SkM1 (green) and Cx32 (red) staining was detected in animals that received the corresponding adenovirus. Nuclei were stained blue using DAPI. Bars represent 50  $\mu$ m.

**Table 1** ECG and local EG measurements during sinus rhythm and ERP recorded during PES

Measurement	Ad-GFP	Ad-SkM1	Ad-Cx32	Ad-SkM1/Cx32
ECG parameters (ms)				
Cycle length	543 $\pm$ 21	535 $\pm$ 18	549 $\pm$ 36	574 $\pm$ 35
PQ	108 $\pm$ 3	114 $\pm$ 6	100 $\pm$ 3	110 $\pm$ 5
QRS	56 $\pm$ 1	46 $\pm$ 1*	51 $\pm$ 2*	46 $\pm$ 2*
QT	224 $\pm$ 5	226 $\pm$ 3	219 $\pm$ 6	232 $\pm$ 8
QTc	305 $\pm$ 6	309 $\pm$ 6	298 $\pm$ 7	307 $\pm$ 6
EG duration (ms)				
LV basal (PS)	21 $\pm$ 0.7	18 $\pm$ 0.9	21 $\pm$ 0.5	21 $\pm$ 0.7
LV anterior (EBZ)	30 $\pm$ 1.1	23 $\pm$ 2.8*	24 $\pm$ 1.0*	21 $\pm$ 0.9*
RV anterior	19 $\pm$ 0.5	20 $\pm$ 0.8	19 $\pm$ 0.5	21 $\pm$ 0.3
ERP (PS) (ms)	159 $\pm$ 2.2	153 $\pm$ 4.8	156 $\pm$ 4.5	156 $\pm$ 8.3
ERP (EBZ) (ms)	167 $\pm$ 5.7	146 $\pm$ 5.6	173 $\pm$ 5.9	163 $\pm$ 4.2

QRS duration and local EG duration in the anterior wall of the left ventricle (LV) incorporating the EBZ are approximately equal to one another in Ad-SkM1, Ad-Cx32, and Ad-SkM1/Cx32-treated animals and are shorter than Ad-GFP. PS, paraseptal site. Ad-GFP,  $n = 22$ ; Ad-SkM1,  $n = 12$ ; Ad-Cx32,  $n = 14$ ; Ad-SkM1/Cx32,  $n = 10$ .

\* $P < 0.05$  vs. Ad-GFP. ERP values did not differ among the four groups. Ad-GFP,  $n = 21$ ; Ad-SkM1,  $n = 11$ ; Ad-Cx32,  $n = 13$ ; Ad-SkM1/Cx32,  $n = 9$ .

Figure 5B). To investigate a potential relationship between infarct size and arrhythmia outcomes, we first pooled the data from all experimental groups. Animals with inducible VT/VF had smaller infarcts than animals without inducible arrhythmias ( $P < 0.05$ ; Figure 5C, left panel). In addition, animals with polymorphic VT/VF had smaller infarcts than animals with monomorphic VT ( $P < 0.05$ ; Figure 5C,

left panel). This observation held as well in a subsequent analysis within the GFP group, in which there was a correlation between smaller infarcts and the presence of polymorphic VT/VF ( $P < 0.05$ ; Figure 5C, right panel). These findings suggest that animals with smaller infarcts are more susceptible to the induction of polymorphic VT/VF.

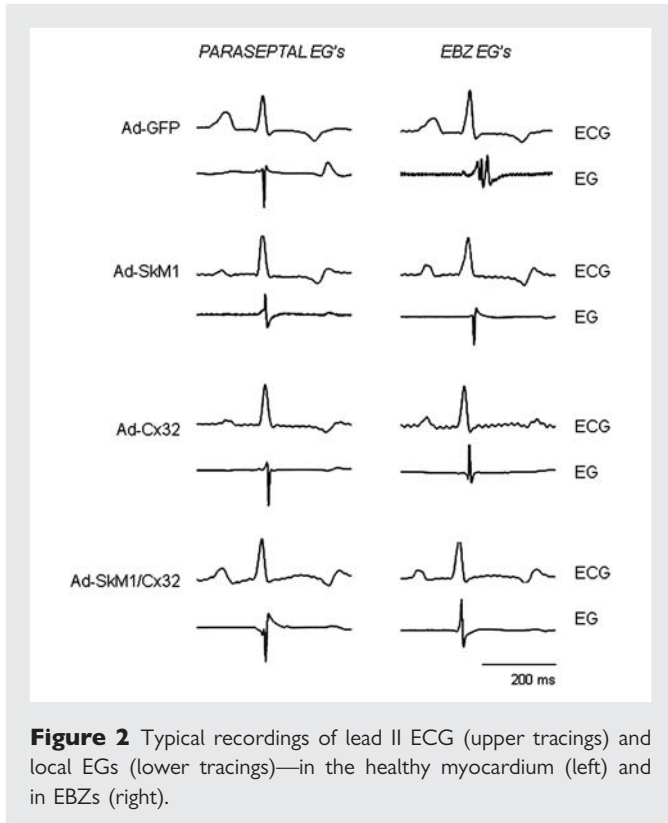


**Figure 2** Typical recordings of lead II ECG (upper tracings) and local EGs (lower tracings)—in the healthy myocardium (left) and in EBZs (right).

### 3.4 In vitro studies

As a functional test of the presence of Cx32, we performed micro-electrode studies to measure the speed of impulse propagation in normal (pH 7.4) and acidic (pH 6.0) environments. Cx32 overexpression increased conduction velocity in normal as well as in low pH settings (Figure 6A and B). As expected, this increase in conduction velocity occurred without concurrent effects on maximum diastolic potential,  $V_{max}$ , or AP duration (APD; Figure 6C).

Functionality of viral SkM1 overexpression has been reported previously<sup>6,7</sup> and additional confirmation of SkM1 functionality in EBZ cells was provided via patch-clamp experiments which are shown in the Supplementary material online; in this study, we primarily compared outcomes of microelectrode studies among the GFP, SkM1, and SkM1/Cx32 groups. The high  $[K]^+$  solution induced significant membrane depolarization and conduction slowing in Ad-GFP-injected preparations ( $P < 0.05$ ; Figure 6D and E). In contrast, Ad-SkM1- and Ad-SkM1/Cx32-injected preparations maintained fast conduction in the high  $[K]^+$  condition. Conduction was similar to baseline (normal  $[K]^+$ ) and significantly faster than in the GFP group (Figure 6D and E). Figure 6F shows that resting potentials and APD were comparable among groups and that all groups exhibited significant membrane depolarization upon the application of high  $[K]^+$ .

In the baseline analysis, outcomes with respect to  $V_{max}$  in the Cx32/SkM1 group ( $P > 0.05$  vs. GFP) were less robust than the SkM1 group ( $P < 0.05$  vs. GFP; Figure 6F). When we compared  $V_{max}$  vs. membrane potential curves, the SkM1 and SkM1/Cx32 groups did not differ

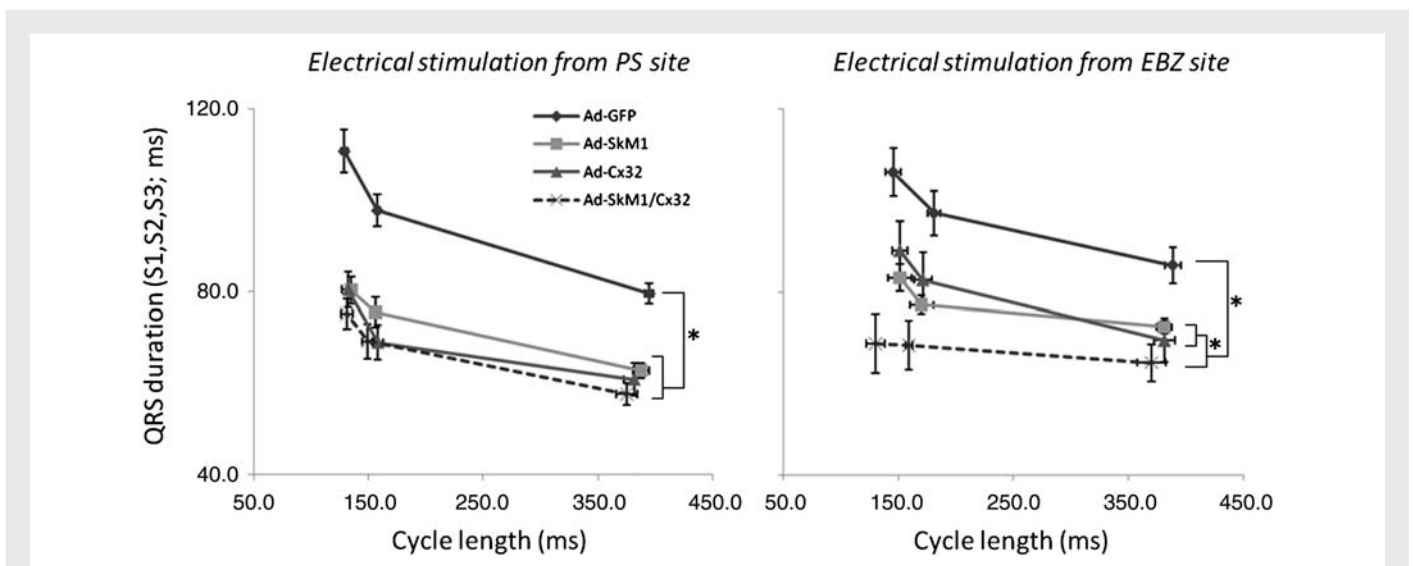


**Figure 3** QRS duration during normal and premature stimulation. (A) Measurements of QRS duration during stimulation from the paraseptal region (PS; left) and from the EBZ/injection region (right). Electrical stimulation was applied as described in Section 2. Some animals could not be included in this analysis because they fibrillated before completion of the protocol (PS: Ad-GFP  $n = 18$ , Ad-SkM1  $n = 10$ , Ad-Cx32  $n = 11$ , and Ad-SkM1/Cx32  $n = 8$ ; EBZ: Ad-GFP  $n = 9$ , Ad-SkM1  $n = 10$ , Ad-Cx32  $n = 8$ , and Ad-SkM1/Cx32  $n = 5$ ). \* $P < 0.05$ .

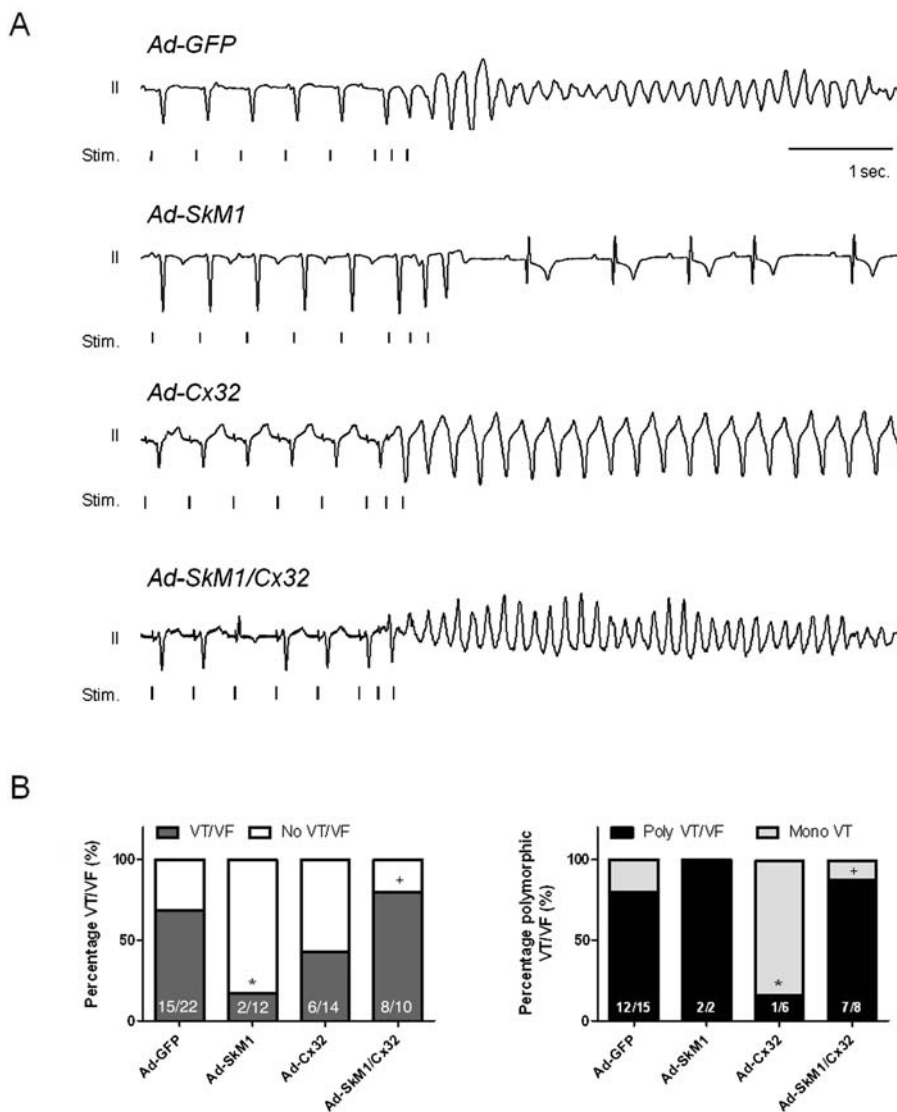


**Figure 4** Incidence and phenotype of induced VT. (A) Typical examples of the phenotypic response to PES. (B) Percentage of inducible VT/VF (left panel) and percentage of polymorphic VT/VF vs. monomorphic VT (right panel). Absolute numbers of animals with VT/VF and total number of animals studied; and the number of animals with monomorphic VT and the total number of animals with VT/VF are presented within the associated bars. \* $P < 0.05$  vs. Ad-GFP; + $P < 0.05$  vs. Ad-SkM1.

statistically from each other ( $P > 0.05$ ), and both had higher values than the GFP group ( $P < 0.05$ ; Figure 6G).

#### 4. Discussion

We recently reported a means to speed/normalize conduction and prevent VT/VF in canine and murine models of infarction and ischaemia/reperfusion, respectively.<sup>6,7</sup> In designing these studies, we understood that in healing infarcts or ischaemic- and reperfused myocardium, there are regions of depolarization resulting in slow conduction and reentry. In both settings SkM1 overexpression resulted in improved Na channel availability.<sup>5,17</sup> The basis for this is that SkM1 channels have positively shifted kinetics of inactivation rendering them primarily open at depolarized potentials at which cardiac Na channels are closed.<sup>18</sup> SkM1 overexpression improved conduction

and reduced the incidence of arrhythmias induced by PES<sup>7</sup> or occurring spontaneously after ischaemia/reperfusion.<sup>8</sup>

The present study adds to the previous findings by comparing outcomes in the healing infarct with SkM1 and with the pH-insensitive connexin, Cx32, and with a combination of SkM1 and Cx32. Our study provides the following new insights in the value of these two gene therapies that speed conduction: (i) the SkM1-based strategy increases  $V_{max}$ , speeds conduction, and reduces the incidence of inducible VT/VF post-myocardial infarction. (ii) The Cx32-based strategy speeds conduction comparably, but rather than being antiarrhythmic, it results in a monomorphic VT (vs. the polymorphic VT/VF in sham dogs and in those few SkM1-treated dogs in which therapy is unsuccessful). Importantly, the change in arrhythmia morphology induced by Cx32 occurs in the setting of an increase in infarct size—highlighting the risks of opening gap junctions during an active

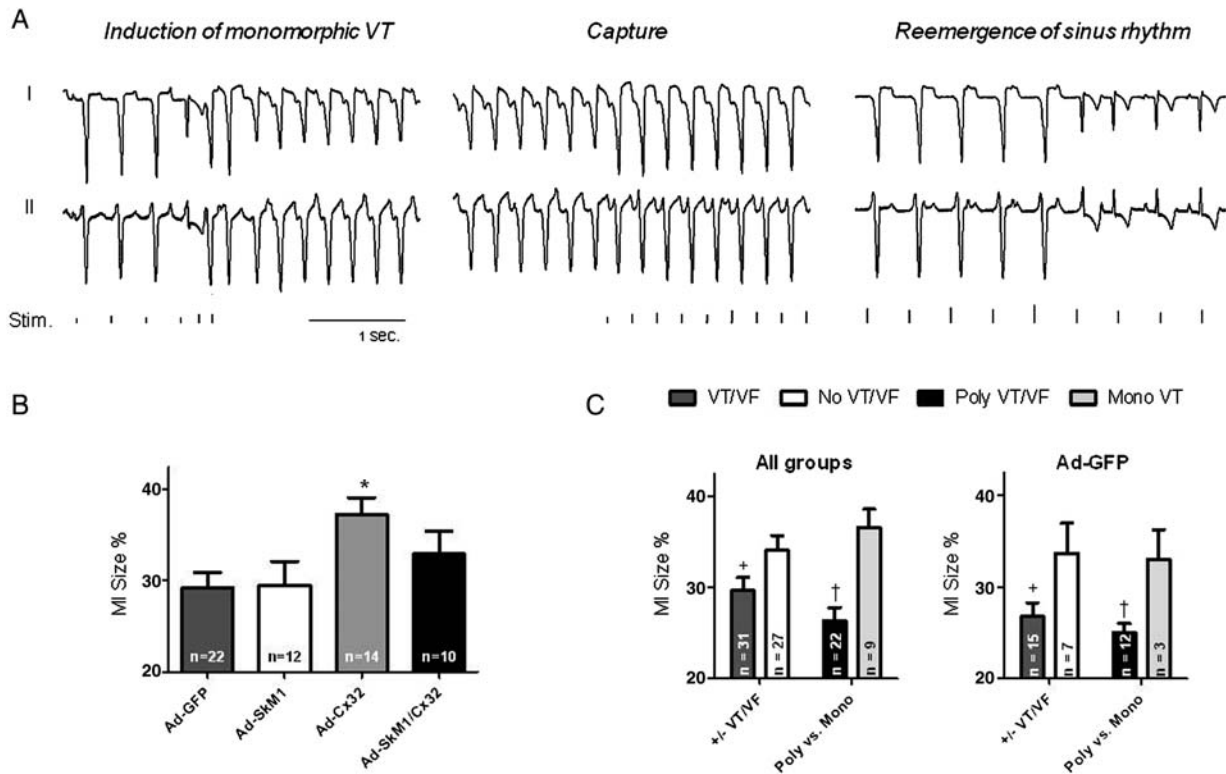


**Figure 5** Response to capture and slowing of pacing rate vs. infarct size. (A) Induction of a monomorphic VT in a Cx32-treated animal (left), initiation of electrical pacing (middle), and reemergence of sinus rhythm (right) which occurred after slowing the rate of electronic pacing. (B) Summary data on infarct sizes. (C) Subanalysis of infarct sizes in animals with and without inducible VT/VF and polymorphic VT/VF vs. monomorphic VT. Shown are the analyses of all animals (left) or the group of GFP-treated animals (right). The number of animals tested within the other groups was too low to allow for a meaningful breakdown and/or statistical analysis (data not shown). \* $P < 0.05$  vs. Ad-GFP; + $P < 0.05$  vs. no VT/VF; † $P < 0.05$  vs. monomorphic VT.

process of infarction. (iii) The SkM1/Cx32-based strategy appears most effective in normalizing QRS duration during premature stimulation, illustrating the potential synergy that may be obtained from combining Cx32 and SkM1. Nevertheless, protection against inducible VT/VF was not obtained.

#### 4.1 Absence of arrhythmia protection in the Cx32 and SkM1/Cx32 groups

The key aspects of outcome in the Cx32 group are the failure to impact on VT/VF incidence (Figure 4), the expression of a monomorphic VT terminated by entrainment (Figure 5A), and the increase in infarct size. Several findings should be taken into consideration here: first, the extent of conduction normalization in the Cx32 group appeared comparable to that in the SkM1 group based on the EG widths (Table 1 and Figure 2), QRS durations during sinus rhythm (Table 1) and premature stimulation (Figure 3), and conduction velocities (Figure 6). Secondly, the larger infarct size in the Cx32 group provides a confounding factor in evaluating the type of arrhythmia that occurred. It is possible that the open gap junction channels in the Cx32 group contributed to enhanced transmission of mediators of injury, thereby creating larger infarcts. It may be that the increase in infarct size in the Cx32 group is associated with more homogeneous tissue damage than is seen in the smaller infarcts which showed

polymorphic VT. A more homogeneous infarct may incorporate a substrate facilitating a large ring of circus movement tachycardia, while the smaller infarcts in the other groups were associated with a more heterogeneous pattern of conduction involving the EBZ and supporting a polymorphic arrhythmia. Prior literature indeed indicates that larger infarcts are positively correlated with monomorphic arrhythmias<sup>19</sup> and that heterogeneous infarcts are particularly prone to polymorphic arrhythmias.<sup>20</sup> Taken together, this suggests that in the setting of Cx32 gene transfer, the combination of normalized conduction and increased infarct size was responsible for the absence of an antiarrhythmic effect while organizing the tachycardia from a polymorphic to a monomorphic phenotype.

That the administration of SkM1 also contravened the expected antiarrhythmic effect of SkM1/Cx32 when the two genes were given together was unexpected, especially in the light of the observation that infarct size was not increased in this group and the arrhythmia remained polymorphic. Although we do not have a definitive explanation for this outcome, there are several possible contributing factors: (i) It is possible that infarct size was not increased due to lower expression of Cx32 in the SkM1/Cx32 group in comparison to the Cx32 group. (ii) The lesser increase in  $V_{max}$  in the SkM1/Cx32 group is consistent with lower expression of SkM1 here than in the SkM1 group. We speculate that a lower  $V_{max}$  might also occur secondary to increased electrotonus (i.e. a space constant

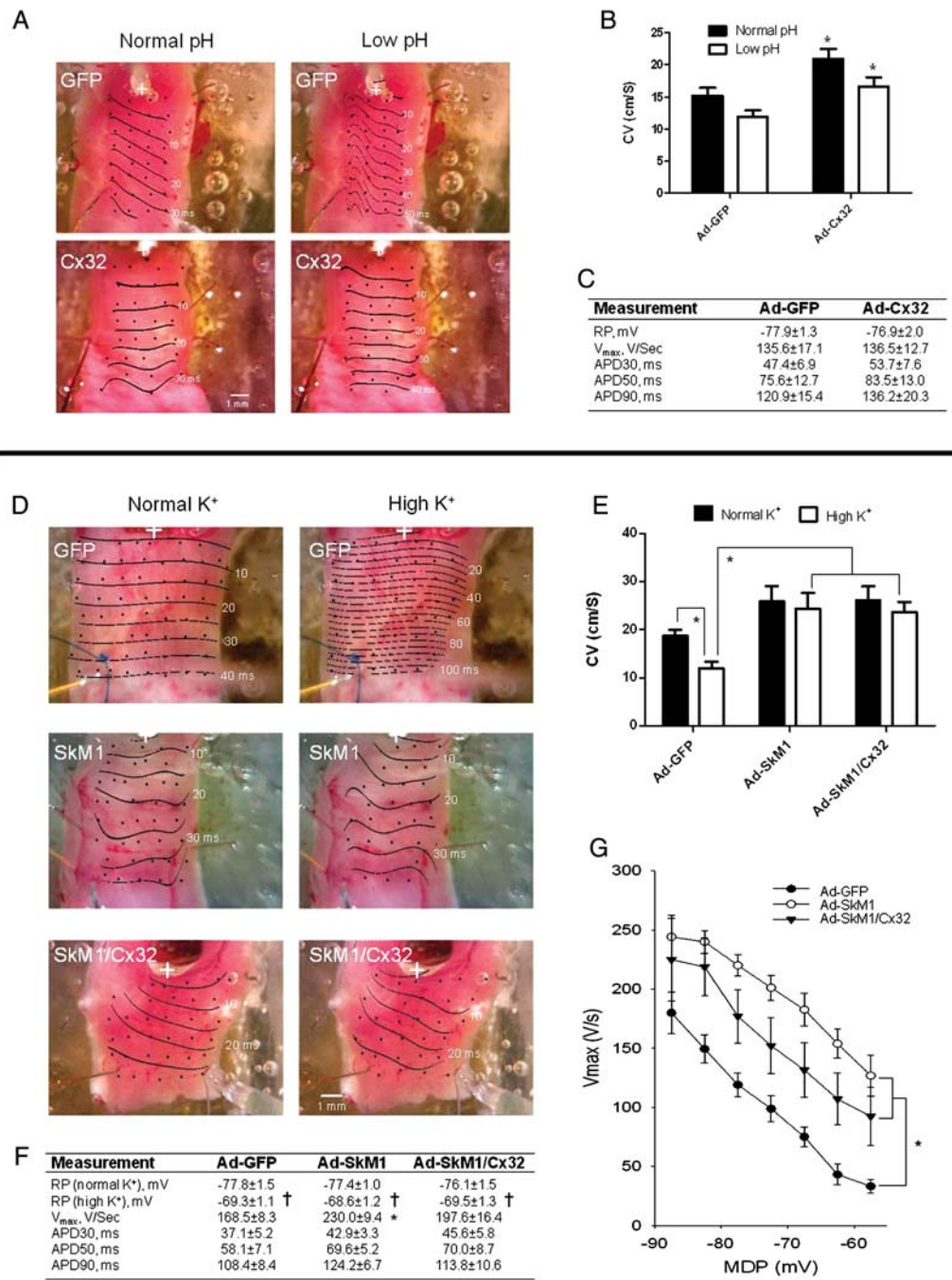


**Figure 6** (Upper) Confirmation of functional presence of Cx32. (A) Representative isochronal maps of EBZ obtained from animals injected with Ad-GFP or Ad-Cx32. As per Section 2, normal pH is 7.4 and low pH is 6.0. (B) Summary data on conduction velocity (CV) indicating faster impulse propagation in the Ad-Cx32 group ( $n = 14$ ) vs. the Ad-GFP group ( $n = 10$ )—both in normal and low pH;  $*P < 0.05$ . (C) Summary data on AP parameters. RP, resting potential; APD, AP duration. (Lower) Comparison of SkM1 and SkM1/Cx32 effects to speed conduction and increase  $V_{max}$ . (D) Typical isochronal maps of EBZ obtained from animals injected with Ad-GFP, Ad-SkM1, or Ad-SkM1/Cx32. In this protocol, extracellular  $K^+$  was increased from 4 to 7 mmol/L (see Section 2). (E) Summary data on CV. (F) Summary data on AP parameters; note that all groups significantly depolarized upon application of high  $K^+$ . (G) Higher membrane responsiveness ( $V_{max}$  vs. MP) curves in Ad-SkM1 and Ad-SkM1/Cx32-injected preparations vs. Ad-GFP. Ad-GFP,  $n = 12$ ; Ad-SkM1,  $n = 8$ ; Ad-SkM1/Cx32,  $n = 10$ . † $P < 0.05$  vs.  $K^+ = 4$  mM/L;  $*P < 0.05$  vs. Ad-GFP.

effect based on Cx32 overexpression). This however must be tested. (iii) Given the comparable speeding of conduction among SkM1 and SkM1/Cx32 groups that occurred in the tissue bath (Figure 6D and E) and the narrower QRS duration in the SkM1/Cx32 group vs. the

SkM1 group upon stimulation from the EBZ site (Figure 3, left panel), it might be that impulse propagation now occurred through pathways that otherwise would have remained silent, creating a polymorphic VT.



Finally, it is noteworthy that the outcome in the Cx32 group is in contrast to that in the murine ischaemia/reperfusion model.<sup>8</sup> Here, SkM1 and Cx32 comparably accelerated conduction and were equally effective in preventing VT/VF. The different outcomes in these two arrhythmia models illustrate the importance of testing antiarrhythmic strategies in diverse settings; they also suggest a more general applicability of SkM1.

## 4.2 Other gene-based strategies to prevent arrhythmias

A variety of gene therapies are being explored with regard to arrhythmias associated with ischaemic heart disease. An effective means to prolong refractoriness has been provided by the Donahue group. They used a dominant negative K-channel to directly prolong repolarization and thereby increase ERP.<sup>21</sup> This approach prevented induction of monomorphic VT<sup>21</sup> and tachy-pacing induced atrial fibrillation.<sup>22</sup> The effectiveness of this approach in preventing polymorphic arrhythmias has not been reported. Although there might be concerns regarding local prolongation of repolarization and potential proarrhythmia, these were not detected in the initial proof-of-concept studies.<sup>21,22</sup> A cell therapy-based approach to carry K-channels, couple to myocytes, and induce post-repolarization refractoriness has also been reported.<sup>23,24</sup>

## 4.3 Study limitations

In experiments on Cx32 gene transfer, the measurements of impulse propagation and infarct size are consistent with the functional presence of Cx32 protein. However, we cannot be certain that some of the outcomes in the Cx32 group(s) derive from potential indirect effects of the gene transfer. To address this issue, further studies are needed to (i) examine potential secondary effects of Cx32 on the expression of other connexins genes (e.g. Cx40, Cx43, and Cx45) and the functional outcome, and (ii) investigate the potential impact on cell geometry.<sup>25</sup> The possibility of functional Cx32 gap junctions between myocytes and fibroblasts is recognized, but this is best studied in cell culture experiments.<sup>26,27</sup> It is likely that this latter eventuality would result in slowing rather than speeding of conduction.

## 4.4 Clinical applicability

The present study is consistent with the proposed applicability of SkM1 as an antiarrhythmic gene therapy while also highlighting some of the risks of improving conduction. Further studies using SkM1 gene transfer will focus on optimizing the delivery vehicle (use of long-term expression vectors may amplify the benefit of an SkM1-based therapy), minimally invasive delivery techniques (e.g. via endovascular or thoracoscopic routes), and application to different types of arrhythmias (e.g. arrhythmias based on chronic ischaemia).

The clinical use of Cx32 gene transfer may be limited due to the potential of this intervention to increase infarct size. It however should be noted that we administered a gene that maintains gap junction channels open at the low pH characterizing ischaemia. It is possible, perhaps likely, that we would have had a beneficial outcome with Cx32 had the gene been delivered at a time when the heart was not undergoing infarction (as was the case in our reperfusion studies in mice<sup>6</sup>). It is also possible that overexpressing Cx43 (a channel which would be closed at low pH and then opened as pH increased to normal) might exert an antiarrhythmic effect. Preliminary

studies using Cx43 overexpression in healed porcine infarcts indeed showed protection against arrhythmia induction.<sup>28</sup> Another aspect of the results with Cx32 in this study and our murine study relates to their implications with regard to antiarrhythmic drug therapies targeted at opening gap junctional channels.<sup>29,30</sup> The suggestion is that such approaches have the potential to be antiarrhythmic as long as there is not the opportunity for channel opening to occur in the setting of an infarct. In a practical sense, this titration may be difficult to achieve. In any event, Cx32 gene transfer might be considered for preventing arrhythmias that are not related to myocardial infarction.

## Supplementary material

Supplementary material is available at *Cardiovascular Research* online.

## Acknowledgements

We thank Eileen Franey for her careful attention to the preparation of the manuscript.

**Conflict of interest:** none declared.

## Funding

This work was supported by grants to M.R.R. from the National Heart, Lung and Blood Institute (HL094410) and the New York State Department of Health (NYSTEM grant CO24344) and an award to R.B.R. from the American Heart Association. G.J.J.B. received grant support from the Netherlands Heart Foundation, the Netherlands Foundation for Cardiovascular Excellence, the Dr Saal van Zwaneberg Foundation, and the Interuniversity Cardiology Institute of the Netherlands.

## References

- Allessie MA, Boyden PA, Camm AJ, Kleber AG, Lab MJ, Legato MJ et al. Pathophysiology and prevention of atrial fibrillation. *Circulation* 2001;**103**:769–777.
- Wit AL, Janse MJ. Experimental models of ventricular tachycardia and fibrillation caused by ischemia and infarction. *Circulation* 1992;**85**:132–142.
- Janse MJ, Wit AL. Electrophysiological mechanisms of ventricular arrhythmias resulting from myocardial ischemia and infarction. *Physiol Rev* 1989;**69**:1049–1169.
- Hennan JK, Swillo RE, Morgan GA, Keith JC Jr, Schaub RG, Smith RP et al. Rotigaptide (zp123) prevents spontaneous ventricular arrhythmias and reduces infarct size during myocardial ischemia/reperfusion injury in open-chest dogs. *J Pharmacol Exp Ther* 2006;**317**:236–243.
- Macia E, Dolmatova E, Cabo C, Sosinsky AZ, Dun W, Coromilas J et al. Characterization of gap junction remodeling in epicardial border zone of healing canine infarcts and electrophysiological effects of partial reversal by rotigaptide. *Circ Arrhythm Electrophysiol* 2011;**4**:344–351.
- Coronel R, Lau DH, Sosunov EA, Janse MJ, Danilo P Jr, Anyukhovskiy EP et al. Cardiac expression of skeletal muscle sodium channels increases longitudinal conduction velocity in the canine 1-week myocardial infarction. *Heart Rhythm* 2010;**7**:1104–1110.
- Lau DH, Clausen C, Sosunov EA, Shlapakova IN, Anyukhovskiy EP, Danilo P Jr et al. Epicardial border zone overexpression of skeletal muscle sodium channel SkM1 normalizes activation, preserves conduction, and suppresses ventricular arrhythmia: an in silico, in vivo, in vitro study. *Circulation* 2009;**119**:19–27.
- Anyukhovskiy EP, Sosunov EA, Kryukova YN, Prestia K, Ozgen N, Rivaud M et al. Expression of skeletal muscle sodium channel (Nav1.4) or connexin32 prevents reperfusion arrhythmias in murine heart. *Cardiovasc Res* 2011;**89**:41–50.
- Penkoske PA, Sobel BE, Corr PB. Disparate electrophysiological alterations accompanying dysrhythmia due to coronary occlusion and reperfusion in the cat. *Circulation* 1978;**58**:1023–1035.
- Garlick PB, Radda GK, Seeley PJ. Studies of acidosis in the ischaemic heart by phosphorus nuclear magnetic resonance. *Biochem J* 1979;**184**:547–554.
- Liu S, Taffet S, Stoner L, Delmar M, Vallano ML, Jalife J. A structural basis for the unequal sensitivity of the major cardiac and liver gap junctions to intracellular acidification: the carboxyl tail length. *Biophys J* 1993;**64**:1422–1433.
- Prestia KA, Sosunov EA, Anyukhovskiy EP, Dolmatova E, Kelly CW, Brink PR et al. Increased cell–cell coupling increases infarct size and does not decrease incidence of ventricular tachycardia in mice. *Front Physiol* 2011;**2**:1.

13. le Marec H, Dangman KH, Danilo P Jr, Rosen MR. An evaluation of automaticity and triggered activity in the canine heart one to four days after myocardial infarction. *Circulation* 1985;**71**:1224–1236.
14. Sosunov EA, Anyukhovskiy EP, Rosen MR. Effects of quinidine on repolarization in canine epicardium, midmyocardium, and endocardium: I. In vitro study. *Circulation* 1997;**96**:4011–4018.
15. Lewandowski R, Procida K, Vaidyanathan R, Coombs W, Jalife J, Nielsen MS *et al*. Rxp-e: a connexin43-binding peptide that prevents action potential propagation block. *Circ Res* 2008;**103**:519–526.
16. Boink GJJ, Lau DH, Sosunov EA, Shlapakova I, Anyukhovskiy EP, Danilo P *et al*. Viral and cell delivery of SkM1 in the post infarct period have differing effects on arrhythmia induction. *Circulation* 2010;**122**:A16485.
17. Protas L, Dun W, Jia Z, Lu J, Bucchi A, Kumari S *et al*. Expression of skeletal but not cardiac Na<sup>+</sup> channel isoform preserves normal conduction in a depolarized cardiac syncytium. *Cardiovasc Res* 2009;**81**:528–535.
18. Wang DW, George AL Jr, Bennett PB. Comparison of heterologously expressed human cardiac and skeletal muscle sodium channels. *Biophys J* 1996;**70**:238–245.
19. Bello D, Fieno DS, Kim RJ, Pereles FS, Passman R, Song G *et al*. Infarct morphology identifies patients with substrate for sustained ventricular tachycardia. *J Am Coll Cardiol* 2005;**45**:1104–1108.
20. Schmidt A, Azevedo CF, Cheng A, Gupta SN, Bluemke DA, Foo TK *et al*. Infarct tissue heterogeneity by magnetic resonance imaging identifies enhanced cardiac arrhythmia susceptibility in patients with left ventricular dysfunction. *Circulation* 2007;**115**:2006–2014.
21. Sasano T, McDonald AD, Kikuchi K, Donahue JK. Molecular ablation of ventricular tachycardia after myocardial infarction. *Nat Med* 2006;**12**:1256–1258.
22. Amit G, Kikuchi K, Greener ID, Yang L, Novack V, Donahue JK. Selective molecular potassium channel blockade prevents atrial fibrillation. *Circulation* 2010;**121**:2263–2270.
23. Feld Y, Melamed-Frank M, Kehat I, Tal D, Marom S, Gepstein L. Electrophysiological modulation of cardiomyocytic tissue by transfected fibroblasts expressing potassium channels: a novel strategy to manipulate excitability. *Circulation* 2002;**105**:522–529.
24. Yankelson L, Feld Y, Bressler-Stramer T, Itzhaki I, Huber I, Gepstein A *et al*. Cell therapy for modification of the myocardial electrophysiological substrate. *Circulation* 2008;**117**:720–731.
25. McCain ML, Desplantez T, Geisse NA, Rothen-Rutishauser B, Oberer H, Parker KK *et al*. Cell-to-cell coupling in engineered pairs of rat ventricular cardiomyocytes: relation between Cx43 immunofluorescence and intercellular electrical conductance. *Am J Physiol Heart Circ Physiol* 2012;**302**:H443–H450.
26. Spach MS, Heidlage JF, Barr RC, Dolber PC. Cell size and communication: role in structural and electrical development and remodeling of the heart. *Heart Rhythm* 2004;**1**:500–515.
27. Gaudesius G, Miragoli M, Thomas SP, Rohr S. Coupling of cardiac electrical activity over extended distances by fibroblasts of cardiac origin. *Circ Res* 2003;**93**:421–428.
28. Greener ID, Sasano T, Igarashi T, Strom M, Pawlowski G, Rosenbaum DS *et al*. Connexin 43 gene transfer improves conduction velocity and reduces ventricular arrhythmia susceptibility. *Heart Rhythm* 2011;**8**:S53–S54.
29. Axelsen LN, Stahlhut M, Mohammed S, Larsen BD, Nielsen MS, Holstein-Rathlou NH *et al*. Identification of ischemia-regulated phosphorylation sites in connexin43: A possible target for the antiarrhythmic peptide analogue rotigaptide (zp123). *J Mol Cell Cardiol* 2006;**40**:790–798.
30. Wiegerinck RF, de Bakker JM, Opthof T, de Jonge N, Kirkels H, Wilms-Schopman FJ *et al*. The effect of enhanced gap junctional conductance on ventricular conduction in explanted hearts from patients with heart failure. *Basic Res Cardiol* 2009;**104**:321–332.